Author's personal copy

Liquids, Theory of: Fermi Liquids ☆

J Spałek, Marian Smoluchowski Institute of Physics, Jagiellonian University, Kraków, Poland and Academic Centre for Materials and Nanotechnology (ACMIN), AGH University of Science and Technology, Kraków, Poland

© 2016 Elsevier Inc. All rights reserved.

Nomenclature

c_s speed of sound in Fermi liquid
c_s^0 speed of sound in electron gas
γ linear specific heat coefficient for quasiparticles
γ_0 linear specific heat coefficient for ideal gas
e electron charge
ε_F bare Fermi energy (for non-interacting particles)
h Planck constant
$\hbar$ Planck constant h-crossed (h divided by 2π)
χ_P Pauli magnetic susceptibility (of electron gas)
χ magnetic susceptibility of Fermi liquid
k wave vector of particle
$\hbar k = p$ momentum of particle
k_F Fermi wave vector
k_B Boltzmann constant
m magnetic moment per site (in dimensionless units)
$\overline{m} = m/n$ magnetic moment per particle
m_0 mass of free electron
$m*$ effective mass of quasiparticle
m_σ spin-dependent effective mass of quasiparticle
μ chemical potential (Fermi energy at $T=0$)
n number of electrons per site (the band filling)
N total particle number
$N_0(\varepsilon)$ density of bare states (both spin directions)
$N(\varepsilon)$ density of quasiparticle states (both spin directions)
$\rho(T)$ electrical resistivity
V system volume
$\rho = N/V$ electron density
v_F Fermi velocity
T temperature (in K)
$T_F \equiv \varepsilon_F/k_B$ Fermi temperature
H_a applied magnetic field (in Tesla)
U magnitude of intraatomic (Hubbard) interaction

☆*Change History*: February 2015. J. Spalek made changes throughout the text.

Author's personal copy

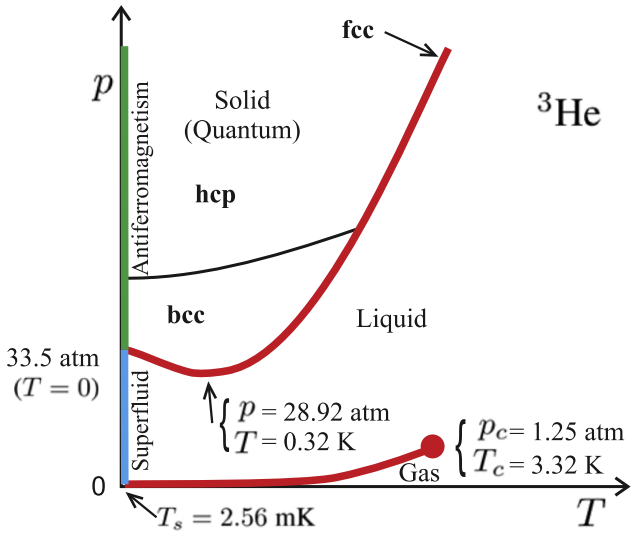

Figure 1 Schematic phase diagram of condensed ^{3}He including its liquid–gas critical point (solid circle). The minimum on the melting curve (Pomeranchuk effect) and the superfluidity (in the mK range) should be noted.

1 Introduction: Quantum Fermionic Liquids

1.1 Basic Characteristics

By Fermi liquid (FL) we mean a quantum many-particle system of interacting fermions (i.e., particles with half-integer spins, such as electrons, neutrons, protons, ^{3}He atoms, and also quarks – all of spins $S=1/2$), which reduces to an (almost) ideal gas of fermions when the same system becomes sufficiently diluted (the particle density becomes sufficiently small). Fermi liquids possesses the same type of phase diagram an pressure (p) – temperature (T) plane as a classical liquid except for two specific features clearly observable for the canonical FL – condensed phase of ^{3}He atoms. First, due to the quantum nature of the particles involved, the zero-point motion prevents its solidification even at temperature $T=0$ and low pressure. Second, FL transformations can take place to the superconducting or/and ordered magnetic states. The last features will not be touched upon here. In other words, we shall talk only about normal Fermi liquids (paramagnetic and non-superfluid). In Figure 1 schematic, but fairly complete, phase diagram for the condensed ^{3}He is provided.

First, we provide some useful formulas for the ideal gas. Namely, as the fermions obey the Pauli exclusion principle, they fill at $T=0$ the momentum $\boldsymbol{p}=\hbar\boldsymbol{k}$ ($\boldsymbol{k}$ is the wave vector of the corresponding matter wave), states of energy $\varepsilon_{\boldsymbol{k}}=\hbar^2\boldsymbol{k}^2/2m_0$ up to the highest occupied level – the Fermi energy ε_F. In the case of an ideal gas with spin $S=1/2$, the value is

$$\varepsilon_F=\frac{\hbar^2k_F^2}{2m_0},\quad \text{with}\quad k_F=\left(3\pi^2\frac{N}{V}\right)^{1/3} \qquad [1]$$

where $\hbar\boldsymbol{k}_F$ is the Fermi momentum, m_0 is the bare (free-atom) mass, and N is the number of particles contained in volume V. For gaseous ^{3}He at normal pressure, one has the velocity of particles at the Fermi energy $v_F=\hbar\boldsymbol{k}_F/m_0\approx 10^4$ cm s^{-1} and the Fermi temperature $T_F=\varepsilon_F/\boldsymbol{k}_B\approx 6.2$ K. The additional characteristic is the density of bare states at the Fermi level, $N_0(\varepsilon_F)$. When counted per atom per one spin direction, it has the value

$$N_0(\varepsilon_F)=\frac{1}{8\pi^2}\frac{V}{N}\frac{2m}{\hbar^2}\left(3\pi^2\frac{N}{V}\right)^{1/3} \qquad [2]$$

In the case of electrons in a solid, one has: $\varepsilon_F\sim 1-10$ eV, $\boldsymbol{k}_F\sim(1\div 2)$ Å^{-1}, and $N_0(\varepsilon_F)\sim 10^{22}$ states eV^{-1}. This is the reason why the particle-energy distribution is regarded as quasicontinuous. However, unlike in liquid ^{3}He, the topology of the Fermi surface for electrons in metals is not spherical and the particle momentum is conserved with accuracy of the order of the inverse-lattice vector $\boldsymbol{G}$. In this context, the liquid ^{3}He can be regarded as a model Fermi liquid on both counts, since it is a truly translationally invariant FL system in the normal state, with spherical Fermi surface according to eqn [1] in the momentum space. Additionally, it is charge neutral as whole atoms are regarded as quantum-mechanical particles compose it.

Author's personal copy

1.2 Basic Definitions

The Fermi liquid theory bears its name from the first phenomenological approach proposed by L.D. Landau (1956–57), which aims to describe the quantum properties of liquid ^{3}He in the normal (non-superfluid) state at low temperatures, $k_B T \ll \varepsilon_F$ ($T \lesssim 1$ K). The spin $S = 1/2$ is that of ^{3}He nucleus, since its $1s^2$ filled electronic shell is spinless. On the other hand, the liquid composed of valence electrons in simple metals: Li, Na, or Cs represents a charged anisotropic FL of electrons coupled to the periodically arranged (much heavier) ions via the electron–lattice coupling. Separate classes of FL represent the neutron stars (their external layers) and the quark–gluon plasma, which compose liquids with relativistic speed of the particles at the Fermi level.

The FL state is a viable concept for three-dimensional systems, whereas one-dimensional systems (fermionic chains, ladders, and nanotubes) are often described as *Tomonaga–Luttinger liquids*. The exact nature of the two-dimensional electronic liquids (e.g., the high-temperature superconductors in the normal state or the quantum Hall liquids) is under extensive investigation, but they are certainly not regarded as Landau Fermi liquids. Also, the three-dimensional systems close to the magnetic or localization instability (quantum critical point) represent non-Landau (*non-Fermi*) liquids, NFL. Therefore, by normal FL (or Landau FL), one understands that it is a three-dimensional quantum liquid composed of interacting fermions with delocalized states and without phase transition in this state induced by either mutual interactions between them or coupling to the lattice, or even when changing the system temperature.

A separate class is formed by the FLs close to the Mott (or Mott–Hubbard) localization; these are called *the almost localized Fermi liquids* (ALFLs) (in the case of ^{3}He, this transition corresponds to the solidification, also included in **Figure 1**). The schematic division of the liquids of fermions, together with the corresponding examples, are listed in **Figure 2**.

1.3 Signatures of the Normal Fermi-Liquid State

The fundamental property of the FL state is the existence of a well-defined reference (gas) of single-particle states with momentum $\boldsymbol{p} = \hbar \boldsymbol{k}$ in the ground and lowest excited states with the energy $\varepsilon_{k\sigma}$, where the spin quantum number is $\sigma = \pm 1$ (note that the z – component of the spin in physical units is $S^z = \hbar\sigma/2$). Those reference states occupy their energy levels $\varepsilon_{k\sigma}$ according to the Fermi distribution

$$n^0_{k\sigma} = \frac{1}{\exp[\beta(\varepsilon_{k\sigma} - \mu)] + 1} \qquad [3]$$

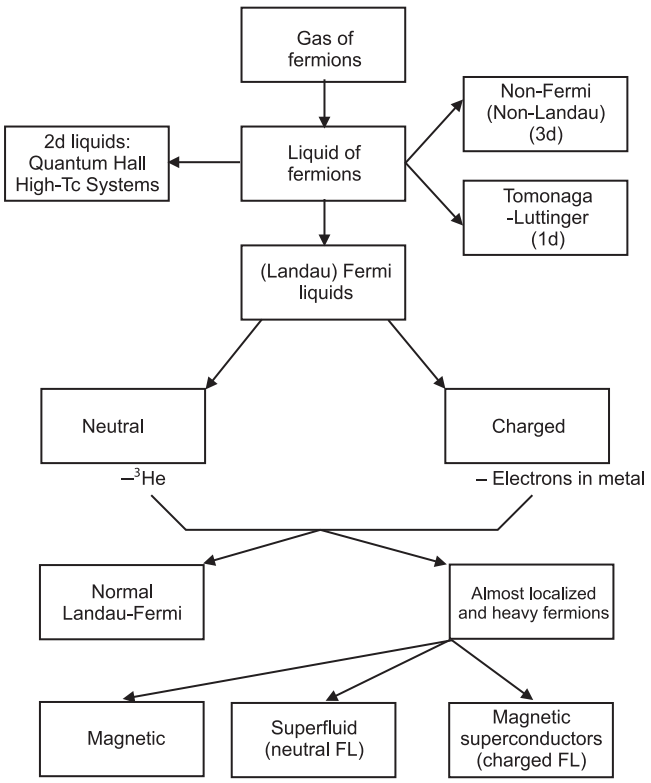

Figure 2 Division of various liquids of fermions and the subdivision of the FLs into various classes.

Author's personal copy

where $\beta=(k_BT)^{-1}$ is the inverse temperature in energy units, and μ is the chemical potential determined from the fact that the total number of particles is conserved, that is, $N=\sum_{k\sigma}n^0_{k\sigma}$. In the ground state, this distribution reduces to the step function $n^0_{k\sigma}=\Theta(\mu-\varepsilon_{k\sigma})$ expressing the Pauli exclusion principle, and μ expresses then the Fermi energy ε_F. The equation $\varepsilon_{k\sigma}=\varepsilon_F$ determines the shape of two (spin-dependent Fermi) surfaces in reciprocal (k) space. In the normal state and in the absence of an applied magnetic field, $\varepsilon_{k\sigma}=\varepsilon_k$, and under this circumstance a single Fermi surface emerges and k_F represents (angle-dependent, in general case) Fermi wave vector. In both solids and liquid ^{3}He the value $k_F\sim 1$ Å^{-1} and this correspond to the Fermi velocity $v_F\equiv p_F/m_0=\hbar k_F/m_0$.

1.3.1 Interaction among particles

The FL concept is particularly useful in the low-temperature regime $T\ll T_F=\varepsilon_F/k_B$, where the interest lies only in describing the thermal (and dynamic) properties of the lowest excited states. In other words, we are interested only in low-temperature properties and gently perturbed by external fields changes with respect to the grand state. In this limit, one is interested in determining the system energy change δE induced by the small change in particle occupancy redistribution $\delta n_{k\sigma}\equiv n_{k\sigma}-n^0_{k\sigma}\ll 1$ (on average), due to both interaction among them, and/or by the thermal excitations (the exact knowledge of the total state energy E is difficult to calculate and even not necessary for the description of low-T properties). In this situation, the interaction in the diluted gas of excited states can be included in the energy δE by making the expansion in terms of the occupation change:

$$\delta E=\sum_{k\sigma}(\varepsilon_k-\mu)\delta n_{k\sigma}+\tfrac{1}{2}\sum_{kk'\sigma\sigma'}f^{\sigma\sigma'}_{kk'}\delta n_{k\sigma}\delta n_{k'\sigma}+\cdots \qquad [4]$$

where $f^{\sigma\sigma'}_{kk'}$ expresses the (generally spin-dependent) density–density interaction between the excited particles, that leads foremostly to the elastic scattering processes at the Fermi surface, as inside it the scattering processes are practically blocked out by the Pauli principle (the possible excited states are blocked by states remaining occupied). It should also to be noted that the bare (without interaction included) energy ε_k is counted from $\mu(=\varepsilon_F$ at $T=0)$. In such formulation, the ground state is regarded as a vacuum state and scattering due to the repulsive interaction (e.g., of Coulomb-type) has the density–density form involving creation of excited occupied state with energy $\varepsilon-\mu\geq 0$ (particles) and the empty states (holes) with $\varepsilon-\mu\leq 0$.

In such approach, there are two subtleties apart from the unknown exact structure of the scattering function $f^{\sigma\sigma'}_{kk'}$. The first is connected with the conservation of particles number, which now takes the form $\sum_{k\sigma}\delta N=0$. In other words, if the single-particle excitations with $\varepsilon_k>\mu$ are regarded as particles ($\delta n_k=+1$), then those with $\varepsilon_k<\mu$ should be regarded as having $\delta n_k=-1$, i.e., as holes. Alternatively, the excitation from the vacuum state requires that if the charge $+e$ is associated with the state $\varepsilon_k>\mu$ and $\delta n_{k\sigma}=1$, then the charge $-e$ has to be associated with the excitation $\varepsilon_k<\mu$, so that the total charge of the ground (vacuum) and the excited states remains zero. This concept bears its origin from the Dirac concept of electrons and holes in relativistic quantum mechanics, which in the present (nonrelativistic) situation does not lead to any peculiarities.

1.3.2 The Entropy of interacting particles ($T\ll T_F$)

The second feature is associated with the determination of δn_k at $T>0$ or equivalently, with the determination of the system entropy. Here, the phenomenology appears in its earnest namely, one assumes that it is taken in the usual form for noninteracting fermions for the number of particles $\{\delta n_{k\sigma}\}$, that is,

$$\delta S=-k_B\sum_{k\sigma}\{\delta n_{k\sigma}\ln\delta n_{k\sigma}+(1-\delta n_{k\sigma})\ln(1-\delta n_{k\sigma})\} \qquad [5]$$

This assumption is justified by adopting the so-called *adiabatic principle* at the beginning: the single-particle (quasiparticle) states in the presence of the interparticle interaction are in a one-to-one correspondence with those for the reference ideal gas. In other words, the number of microconfigurations in the interacting system does not change, nor does the configurational entropy. This theorem finds its microscopic justification through the Luttinger theorem (1960): the Fermi volume (i.e., the number of states encompassed by in k-space by radius k_F at $T=0$) does not depend on the interaction magnitude as long as the system does not undergo either magnetic or superconducting or delocalization–localization transition. This theorem implies that the occupation number ($\delta n_{k\sigma}$) can change, but the Fermi ridge (discontinuity) position in k space does not. It amounts to saying that the number of available states for electrons in the states $\varepsilon_k>\mu$ is the same as that for the holes (with $\varepsilon_k<\mu$).

1.3.3 Quasiparticles

By writing down the total energy in the form

$$\delta E=\sum_{k\sigma}\left\{\varepsilon_{k\sigma}-\mu+\frac{1}{2}\sum_{k'\sigma'}f^{\sigma\sigma'}_{kk'}\delta n_{k'\sigma}\right\}\delta n_{k\sigma}\equiv\sum_{k\sigma}E_{k\sigma}\delta n_{k\sigma} \qquad [6]$$

Author's personal copy

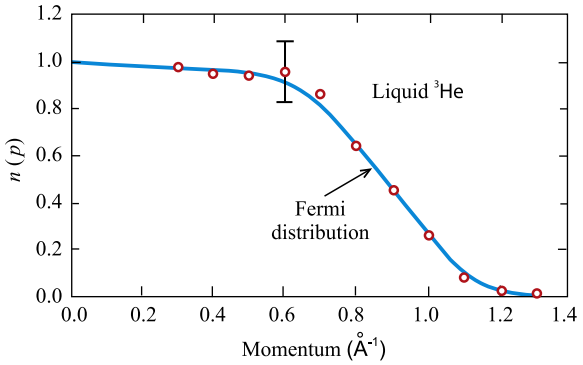

Figure 3 The Fermi distribution for liquid^3 He atoms at $T=0.37$ K and ambient pressure. (After Mook, H.A., 1985. Momentum distribution of ^{3}He. Physical Review Letters 55, 2452).

the energy $E_{k\sigma}$ of the quasiparticle can be defined. This amounts to saying that the effective single-particle energies are well defined. In effect, the distribution [3] for quasiparticles can be redefined (by minimizing the free energy $\delta F=\delta E-T\delta S$), that is, with respect to $\{\delta n_{k\sigma}\}$, with the replacement $\varepsilon_{k\sigma}-\mu\rightarrow E_{k\sigma}$. **Figure 3** provides the statistical distribution function $n(p)\equiv n_{p\sigma}$ for liquid ^{3}He obtained from the neutron scattering experiment of Mook (1985). It can be seen that the Fermi distribution function describes the quasiparticle states well, but with the Fermi temperature $T_F=1.8$ K and the energy given by $E_k=p^2/2\,m^*$, where now $m^*\approx 3m_0$ is the effective mass of ^{3}He atoms in the FL state at $T=0.37$ K. The Fermi temperature is also renormalized by the factor $T_F=(m_0/m^*)T_F^0$, where $T_F^0=\varepsilon_F/k_B$ is the corresponding quantity for ^{3}He gas of the same density. So, the interaction changes both the mass and the Fermi energy to the same extent for all particles (i.e., not only those close to $\boldsymbol{k}_F$). Note that the mass enhancement factor m^*/m_0 is not small and therefore cannot be regarded as a small perturbation of its initial value m_0. It represents an effective, *renormalized* mass due to the interparticle interaction. In other words, the mass increases in the milieu of all other particles due to a repulsive interaction between them. Parenthetically, this means that the concept of mass in quantum physics is not invariant to the same extent as in the classical physics.

1.3.4 Electrons in metal as quasiparticles

The states of electrons in a metal are probed by exciting them by photons in the photoelectron emission from the solid. To describe such a process, one has to know the so-called spectral density function $A_{k\sigma}(\omega)$ describing microscopically the form of the system energy spectrum when extracting (or adding) one electron with momentum $\hbar\boldsymbol{k}$ and the energy ω. $A_{k\sigma}(\omega)$ is, in turn, defined as

$$A_{k\sigma}(\omega)=-\frac{1}{\pi}\mathrm{Im}G_{k\sigma}(\omega)\equiv-\frac{1}{\pi}\mathrm{Im}\frac{1}{\omega-E_{k\sigma}+i\sum_{\sigma}''(\omega)} \qquad [7]$$

where $G_{k\sigma}(\omega)$ is the retarded single-particle Green function for the quasiparticle. The quantity $\sum_{\sigma}''(\omega)$ represents the imaginary part of the self-energy $\sum_{\sigma}$ and for a three-dimensional FL is given by

$$\sum_{\sigma}''(\omega)=\beta\omega^2,\quad \beta=const. \qquad [8]$$

The real part of the self-energy is included in $E_{k\sigma}$ (replacing in microscopic theory the phenomenological part $\sim f_{kk'}$) and leads to the mass enhancement; in the simplest case: $E_k=(m_0/m^*)\varepsilon_k$, where ε_k is the corresponding energy of particle in gas of the same density.

The function $A_{k\sigma}(\omega)$ is of fundamental importance for the many-particle system. This is because the density of states $N(\omega)$ and the statistical distribution function $n_{k\sigma}$ are derived from it, namely,

$$N(\omega)=\sum_{k}A_{k\sigma}(\omega);\quad n_{k\sigma}=\int d\omega A_{k\sigma}(\omega) \qquad [9]$$

where the integration is over allowed values of energy of the system (e.g., the band width or the cutoff energy). In the paramagnetic systems, the spin subscript is dropped; sometimes $A_{k\sigma}(\omega)$ is defined by summing up over $\sigma=\pm 1$. The photoemission intensity, that is, the number of electrons emitted in the direction $\boldsymbol{k}$ with the energy ω is given by

$$I_k(\omega)=I_0\int d\omega' A_k(\omega')\,n(\omega')\,R(\omega') \qquad [10]$$

where $R(\omega-\omega')$ is the so-called resolution (instrument) function (usually taken in the Gaussian form), $n(\omega)$ is the Fermi factor: $n(\omega)=[\exp(\beta\omega)+1]^{-1}$, with $\omega=0$ representing the Fermi energy (I_0 is the normalization constant). **Figure 4** provides an

Author's personal copy

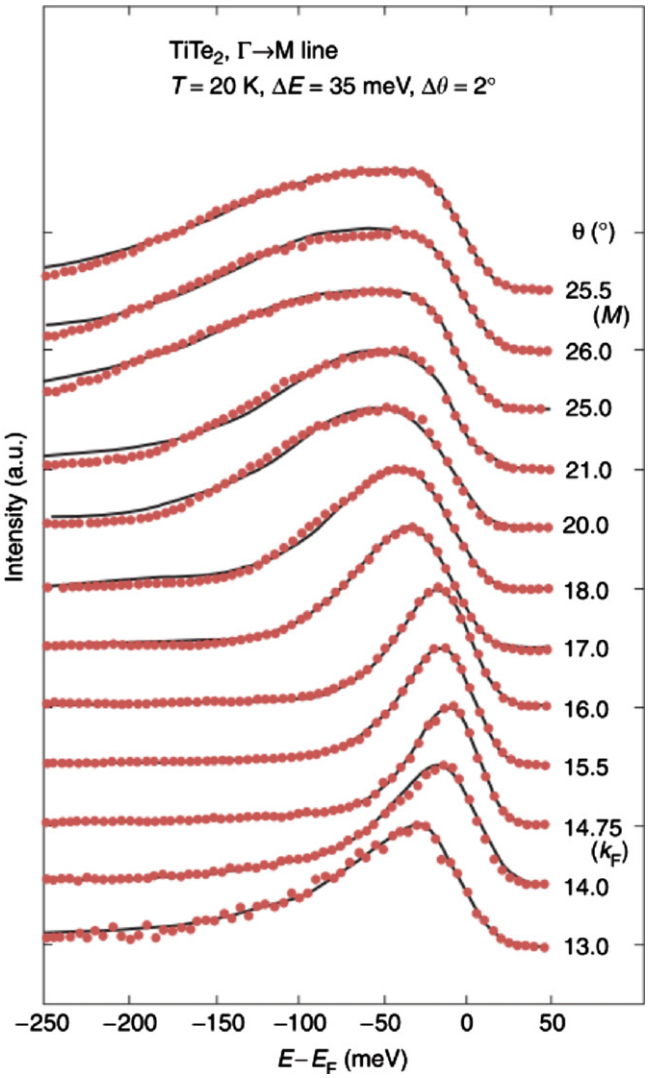

Figure 4 Photoemission spectra for a quasi-two-dimensional metal $TiTe_2$ along the $\Gamma \rightarrow M$ line (from bottom to top). The solid line represents the Fermi-liquid fit of the first equation of [9] to the data. The spectra are normalized to the same maximum height. After Allen, J.W., Gweon, G.-H., Claessen, R., Matho, K., 1995. Fermi liquids and non-Fermi liquids: The view from photoemission. Journal of the Physics and Chemistry of Solids 56, 1849.

exemplary angle-resolved photoemission spectrum (ARPES) with the quasiparticle peak dispersing as the regime of energies is probed with $E_{\boldsymbol{k}} < \mu$; the angle θ describes the angle at which the photoelectron is emitted, and determines the wave vector $\boldsymbol{k}_{\|}$ in this quasi-two-dimensional metal and in turn, the particle energy. The dispersion relation for quasiparticles is linear when $E_{\boldsymbol{k}} \rightarrow \mu$, i.e., $E_{\boldsymbol{k}} - \mu = \hbar \boldsymbol{v}_F \cdot (\boldsymbol{k} - \boldsymbol{k}_F)$. More advanced angle-resolved techniques leads to the determination of the explicit form of dispersion relation, i.e., the part with $E_{\boldsymbol{k}} - \mu < 0$ at is particularly useful for quasi-two-dimensional high temperature superconductors. This is because for two dimensional systems in plane component of $k = k_{\|}$ represents the whole particle momentum and thus $E_{\boldsymbol{k}_{\|}} \equiv E_{\boldsymbol{k}'}$.

2 Properties at Low Temperatures

A brief description of the properties at low T follows. For that, first the function $f_{\boldsymbol{k}\boldsymbol{k}'}^{\sigma\sigma'}$ has to be specified. Namely, if elastic scattering processes at the Fermi-surface-only are included, then one can postulate that $f_{\boldsymbol{k}\boldsymbol{k}'}^{\sigma\sigma'} = f_{\boldsymbol{k}\boldsymbol{k}'}^{\sigma\sigma}(\boldsymbol{k}_F \cdot \boldsymbol{k}_F'/k_F^2)$, that is, the elastic scattering processes depend only on the relative angle between the respective momenta. Additionally, one can extend the form to the explicitly spin-dependent form:

$$f_{\boldsymbol{k}\boldsymbol{k}'}^{\sigma\sigma'} = f^s\left(\boldsymbol{k} \cdot \boldsymbol{k}'/k_F^2\right) + \sigma \cdot \sigma' f^a\left(\boldsymbol{k} \cdot \boldsymbol{k}'/k_F^2\right) \qquad [11]$$

Author's personal copy

where σ, $\sigma' = \pm 1$ is the spin-quantum number and $\boldsymbol{k} = \boldsymbol{k}' = \boldsymbol{k}_F$. The form [11] defines the spin-symmetric ($f^s = \frac{1}{2}(f^{\uparrow\uparrow} + f^{\uparrow\downarrow})$) and the antisymmetric ($f^a = \frac{1}{2}(f^{\uparrow\uparrow} - f^{\uparrow\downarrow})$) functions in the situation when the spin–spin interaction is rotationally invariant (e.g., when we neglect the spin–orbit interaction). Additionally, introducing $\theta \equiv \boldsymbol{k} \cdot \boldsymbol{k}'/k_F^2$, the functions can be expanded in terms of the Legendre polynomials $P_l(\cos\theta)$, that is,

$$f_{\boldsymbol{k}\boldsymbol{k}'}^{s,a} = \sum_{l=0}^{\infty} f_l^{s,a} P_l(\cos\theta) \tag{12}$$

where coefficients with given angular momentum (are defined as)

$$f_l^{s,a} = (2l+1) \int_{-1}^{+1} dx P_l(x) f^{s,a}(x) \tag{13}$$

and represented the partial spherical-wave amplitudes. The ingenuity of this approach is rooted in the circumstance, realized only *a posteriori*, that all the principal physical properties can be expressed in terms of a few parameters (f_0^s, f_1^s, and f_1^a). These properties can be expressed in terms of the dimensionless interaction parameters $F_l^{s,a} \equiv N(0) F_l^{s,a}$, where $N(0)$ is the density of states at the Fermi level including both spin directions and is defined by

$$N(\mu = 0) = \sum_{\boldsymbol{k}\sigma} \delta(E_{\boldsymbol{k}} - \mu) = -2(2\pi)^{-3} \int d^3\boldsymbol{k} (\partial/\partial E_{\boldsymbol{k}}) \theta(\mu - E_{\boldsymbol{k}}) = v_F(m^*/\hbar^3\pi^2) \tag{14}$$

The last expression is valid for linearized dispersion relation: $E_{\boldsymbol{k}} - \mu = \hbar v_F(k_F - k) \equiv (p_F/m^*)(p_F - p)$.

2.1 Summary of Properties

1. Effective mass enhancement at $T = 0$,

$$m^* = m_0 \left(1 + \frac{1}{3} F_1^s\right) \tag{15}$$

where m_0 is the bare mass (the band-theory mass for the case of electrons).

2. Bulk compressibility of the FL system at $T = 0$,

$$\kappa \equiv -\frac{1}{V} \frac{\partial V}{\partial p} = \frac{\rho^2}{V} \frac{\partial \mu}{\partial N} = \frac{\rho^2}{V} \frac{1 + F_0^s}{N(0)} \equiv \kappa_0 \frac{1 + F_0^s}{N(0)} \tag{16}$$

where $\rho \equiv dN/dV$ is the particle density at a given volume; associated with this quantity is the sound velocity v_s, which is $v_s^2 = p_F^2/(3m_0/m^*)(1 + F_0^s)$.

3. Paramagnetic susceptibility at $T = 0$ is enhanced in the following manner:

$$\chi(0) \equiv \left(\frac{\partial M}{\partial H_a}\right)_0 = \frac{1}{4}(g\mu_B)^2 N(0) \frac{1}{1 + F_0^a} \equiv \chi_p \frac{m^*/m_0}{1 + F_0^a} \tag{17}$$

where g is the Lande factor and $(\partial M/\partial H_a)_0$ expresses the magnetic susceptibility as the ratio of magnetization to the magnitude of the (small) applied magnetic field creating it. $\chi_p = \frac{1}{2}(g\mu_B)^2 N_0(0)$ represents the Pauli susceptibility of the Fermi gas. At $T > 0$, the susceptibility takes the form $\chi(T) = \chi(0)(1 + \tilde{a}T^2)$, where $\tilde{a}$ is a constant, which can be obtained from the low-T expansion.

4. Electrical resistivity of the electron fluid can be represented by the formula $\rho = m^*/(n_c e^2 \tau)$, where n_c is the carrier concentration, $e = |e|$ is the carrier charge, and τ is the lifetime for scattering due to the inter-particle interactions (Baber–Landau–Pomeranchuk)

$$1/\tau \sim m^* T^2 \tag{18}$$

So the resistivity can be described by $\rho(T) = AT^2$, with $A \sim \gamma(0)^2$, where $\gamma(0)$ is the linear specific heat coefficient $\gamma(0) = (\pi^2/3) k_B^2 N(0)$. In the case of neutral FL, this inverse relaxation time determines the viscosity.

Author's personal copy

5. Specific heat has both the contributions due to single-particle excitations, $\sim\gamma(0)T$ and that due to the collective spin fluctuations; the latter are reflected in the simplest case as a maximum in the dynamic susceptibility $\chi(q,\omega)$ at $q=\omega=0$. In effect,

$$C(T)=\gamma(0)T+\delta T^3\ln(T/T_{sf}) \qquad [19]$$

where $\gamma(0)=m^*p_F/(3\hbar^3)\equiv\gamma_0(0)m^*/m_0$, and δ and T_{sf} are characteristics of the collective spin fluctuation spectrum.

6. The Wilson ratio of the extrapolated values, $R_w\equiv\chi(0)/\gamma(0)$, describes the relative strength of magnetic and charge excitations. For $R_w\gg1$ the system is close to the ferromagnetic stability ($F_0^a\to-1$); in the opposite situation ($F_0^a\to0$) the Wilson ratio for the Fermi liquid is close to that for the Fermi gas (is an universal number $3(g\mu_B)^2/(2\pi^2k_B^2)$).

2.2 Collective Excitations

Apart from the paramagnetic spin fluctuations, there is a specific collective excitation of the FL – the zero sound. It appears for frequencies, for which $\omega\gg\tau^{-1}$, that is, in the collisionless regime for quasiparticles. The role of the restoring force during the propagation of such density fluctuations is provided by the averaged self-consistent field of the remaining particles in the system. In such a nomenclature, the complementary hydrodynamic (collision-dominated) regime corresponds to the sound propagation for $\omega\ll\tau^{-1}$. The density oscillations in the last regime correspond to first-sound propagation in a liquid, which can be identified with damped oscillation, the ordinary sound.

Explicitly, the ordinary (low-frequency) sound for ($\omega\tau\ll1$) propagates with the velocity

$$c_s=\left(\kappa m^*\rho\right)^{-1/2}\equiv c_s^0\,\frac{1+F_0^s}{1+\frac{1}{3}F_1^s}$$

whereas the zero-sound (at high-frequency, $\omega\tau\gg1$) has roughly the value $u\cong\sqrt{3}c_s$. Note, that in the expression for the sound velocities the third constant (F_0^s) appears for the first time, in additional to F_0^a and F_1^s.

Apart from those excitations, there are electron–hole and plasmon excitations, for elaboration of which the reader is advised to consult more specialized texts (see Further Reading section). The same remark applies to the discussion of other nonequilibrium and transport properties of Fermi liquids.

2.3 Liqiud ^{3}He as a Test Case

As one can see from eqns [15]–[17], one can determine the three parameters F_1^s, F_s^0, and F_a^0 by measuring respectively the linear specific heat, bulk compressibility, and paramagnetic susceptibility for given particle density N/V (i.e., for given pressure) for which one calculates the Fermi momentum $p_F=\hbar k_F$ and the density of states according to corresponding formulas for the ideal gas. In **Table 1** we display the values of those parameters as a function of pressure. Note that the values of determined parameter can be taken as input values to determine the explicit values of other (e.g., dynamic) properties and thus, to test the theory mutual consistency, though such test has not been carried out so far. Also, the parameter values are not small, as even when $F_0^a\to-1$, the magnetic susceptibility is singular and reaches *the Stoner threshold* for a quantum transition to ferromagnetism. On the other hand, the effective mass can become large ($m^*/m_0\sim6$ at the solidification point of heavy fermions m^*/m_0 can reach the value 10^2 or even larger, see below).

3 Unconventional Fermi Liquids

A brief summary of the Landau approach to the Fermi liquids is as follows. The expansion of the system energy (internal energy for $T<0$) does not start with a microscopic Hamiltonian, although it can be justified in the manner. This approach conveys physics even without the explicitly known Hamiltonian and still can provide predictions concerning an overall behavior of the system as a function of pressure and/or temperature if only $\boldsymbol{k}_BT\ll\mu$. So, it minimally provides a semiquantitative rationalization of the basic macroscopic properties for fermionic systems in the liquid or the interacting gas states, in a single-phase state, i.e., when there are no phase transitions and/or classical/quantum critical points encountered. The inclusions of the last features requires generalization of the Landau–Fermi-liquid concept we overview briefly next.

A nonstandard behavior is to be expected when a normal FL undergoes a phase transition. As liquids which undergo the superconducting or superfluid transitions are discussed elsewhere in this encyclopedia, the focus here is on the solidification of ^{3}He and the Mott–Hubbard localization of an almost localized electron liquid. **Figure 5** provides the molar pressure dependence of $\gamma(0)=(\pi^2/3)k_B^2N(0)$, as well as the mass enhancement m^*/m_0 for ^{3}He calculated from the relation $\gamma(0)=\gamma_0(m^*/m_0)$, where $\gamma_0=(\pi^2/3)k_B^2N_0(0)$, and $N_0(0)$ represents the corresponding density of states for an ideal ^{3}He gas (of the same density). Parenthetically, the density of states in FL state, $N(0)$, is also enhanced, $N(0)=N_0(0)(m^*/m_0)$. As the liquid approaches the solidification threshold, that is, freezing of atoms into a lattice, the quasiparticle mass doubles. At the highest pressure (~36 bars), the system solidifies via a discontinuous transition. This is regarded as a canonical case of the Mott transition from F-L to an atomic

Table 1 Fundamental properties of liquid ^{3}He versus pressure and the corresponding values of the three Landau parameters: F_0^s, F_1^s, and F_0^a (After: Dobb, 2000)

Pressure p *(MPa)*	*Molar volume* V_{mol} *($cm^3\ mol^{-1}$)*	*Linear specific-heat* γ *(K^{-1})*	*Mass renormalization* m^*/m_0	*Fermi momentum* $10^{25}\ p_F$ *(kg m s^{-1})*	*Fermi velocity* v_F *(m s^{-1})*	*Sound velocity* c_s *(m s^{-1})*	*Fermi temperature* T_F *(K)*	*Landau parameters*		
								F_0^s	F_1^s	$-F_0^a$
0	36.84	2.78	2.80	8.28	59.0	182.9	1.771	9.30	5.39	0.698
0.3	33.95	2.98	3.16	8.51	53.8	227.5	1.657	15.98	6.49	0.724
0.6	32.03	3.16	3.48	8.67	49.7	259.7	1.526	22.54	7.45	0.734
0.9	30.71	3.32	3.77	8.80	46.6	285.9	1.485	28.95	8.31	0.741
1.2	29.71	3.48	4.03	8.89	44.1	308.0	1.418	35.37	9.09	0.746
1.5	28.89	3.62	4.28	8.98	41.9	327.1	1.362	41.75	9.85	0.751
1.8	28.18	3.77	4.53	9.05	39.9	345.0	1.307	48.51	10.60	0.754
2.1	27.55	3.92	4.78	9.12	38.1	360.5	1.258	55.19	11.34	0.756
2.4	27.01	4.06	5.02	9.18	36.5	375.1	1.214	62.05	12.07	0.757
2.7	26.56	4.21	5.26	9.23	35.0	389.3	1.1714	69.37	12.79	0.757
3.0	26.17	4.36	5.50	9.28	33.7	403.0	1.132	77.08	13.50	0.756
3.3	25.75	4.50	5.74	9.33	32.5	415.9	1.096	84.85	14.21	0.756
3.439	25.50	4.56	5.84	9.36	31.9	421.7	1.083	88.37	14.56	0.756

Author's personal copy

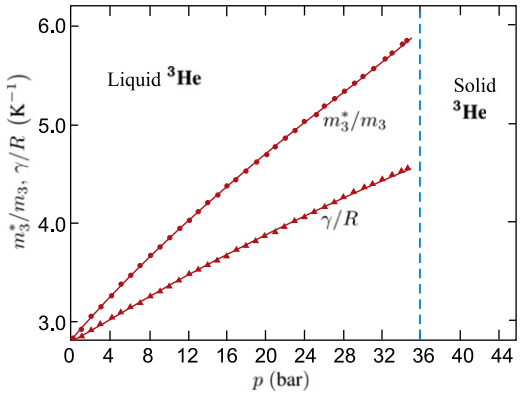

Figure 5 Pressure dependence of the linear specific-heat coefficient $\gamma(0)$ (in units of the gas constant R) and the effective mass enhancement m^*/m_0 of the ^{3}He atoms in the liquid state (top), when approaching the solidification. (After Greywall, D.S., 1986. ^{3}He specific heat and thermometry at millikelvin temperatures. Physical Review B 33, 7520).

lattice at spin 1/2 particles. At the transition the Fermi surface disappears, since $m^*/m_0 \to \infty$ if the transition were continuous. Also, due to a weak van der Waals binding of atoms into a lattice and a large zero-point motion of atoms as quantum particles, a number of phases is possible under applied pressure.

3.1 Heavy-Electron Systems

Even more spectacular effective mass enhancement is also observed in the heavy-electron systems, which compose intermetallic compounds involving itinerant $4f$ or $5f$ electrons, for example, $CeAl_3$, UPt_3, UBe_{13}, and many others. The effective masses m^* encountered there can reach $\sim 10^2\, m_0$.

In **Figure 6** we provide the collected data for the principal characteristic for $CeAl_3$ and related systems. Note that value of $\gamma \simeq 1600$ mJ mol^{-1} K^{-2}, the value of χ enhanced also strongly and finite as $T \to 0$, the signature of a paramagnetic state. Additionally, the T^2 dependence of the resistivity is clearly seen. This system represents also a canonical system of a normal Landau Fermi liquid with enormous effective mass of the carriers. The original form initial $4f$ electrons of Ce^{3+} ions must lead to such huge enhancement of $\gamma(0)$, since the isostructural compound. $LaAl_3$ does not possess any of the above characteristics.

In **Figure 7**, the molar specific heat data for the moderately heavy-fermion compound $CeRu_2Si_2$ is presented. The extrapolated value of $\gamma(0) = 355$ mJ K^{-2} mol^{-1} has been subtracted from the C/T data. The heavy mass of these quasielectrons is characterized by new characteristic temperature replacing the Fermi temperature $T_F \equiv \mu/k_B$, which is often called *the effective Kondo (coherence) temperature* $T_K \equiv \pi^2 R/3\gamma$, which characterizes roughly the bandwidth for these very heavy quasiparticle states. The solid curve represents the second term of the expression [19] divided by T. The heavy masses are associated, in this case, with the hybridized $4f^1$ states due to the Ce^{3+} ions with the conduction states, and the intraatomic Coulomb interaction for the $4f^2$ configuration is large, so the f-states can become itinerant only when the valency is slightly larger than Ce^{3+} ($4f^{1-\varepsilon}$ configuration with $\varepsilon \lesssim 0.1$). In other words, a small number of holes in the originally atomic $4f^1$ configuration causes the almost localized behavior when these electrons additionally hybridize with the extended valence (band) states of, for example, $5d$–$6s$ type.

The Fermi liquid nature of the compounds for $T \lesssim T_K$ is evidenced further in the behavior of the resistivity $\rho(T) = \rho_0 + AT^2$, as well as by the Wilson ratio R_w close to the value for electron gas. The two observations are displayed in **Figures 8** and **9**, respectively. The straight line in **Figure 8** illustrates the relation $A \sim \gamma(0)^2$, whereas that in **Figure 9** corresponds to a Fermi gas. So, indeed, the concept of very heavy quasiparticles in a very narrow band of hybridized $4f$-conduction band states is applicable even in these extreme situation.

3.2 Almost Localized Systems and Mott–Hubbard localization

As said above, the original Landau theory does not encompass the situation of quantum freezing of the Fermi liquid when, for example, strong enough repulsive interaction among particles forces them to localize into the set lattice states. This is the case of Mott or Mott–Hubbard transition, the latter taking place in the case of lattice fermions.

Under these circumstances, a proper language of description starts with the microscopic Hubbard model (or Anderson-lattice model for hybridized systems), where a short-range type interaction among almost atomic states involves all the system electrons as the whole system undergoes a phase transition. This description is based on starting form a complementary language (atomic limit), whereas the Landau–Fermi liquid concept is based starting from the electron–gas concept. Below we summarize the properties obtained based on the Gutzwiller approximation for the Hubbard model and discuss it subsequently in quasiparticle terms. We assume that we have one state and one electron per atom. The picture is of a mean-field type within the frame of theory of phase transitions.

Author's personal copy

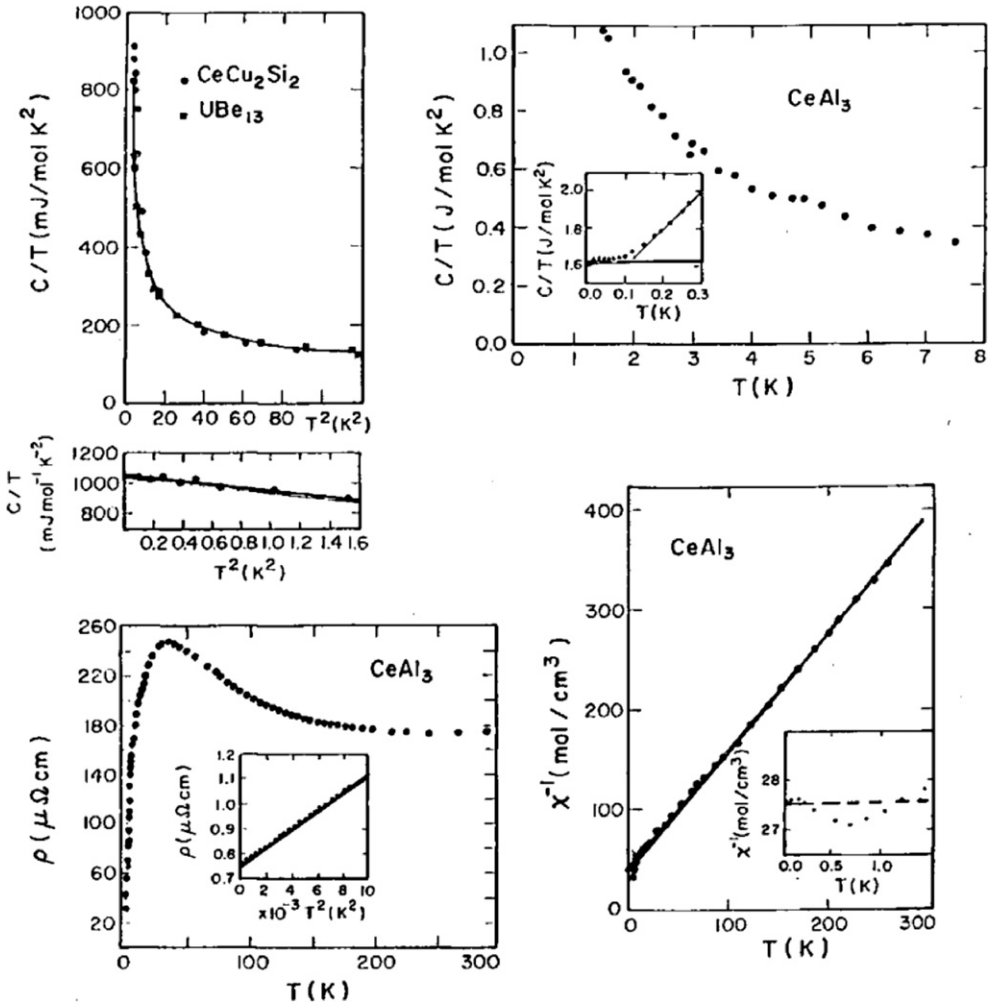

Figure 6 Fundamental electronic properties of heavy fermions $CeAl_3$, UBe_{13}, and $CeCu_2Si_2$. The straight lines are guide to eye to underline the Fermi-liquid temperature deendences (see in particular the insets). Clockwise from left top: linear specific heat coefficient C/T for $CeCu_2Si_2$, UBe_{13}, and $CeAl_3$; inverse magnetic susceptibility showing the evolution with the decreasing T from the Curie–Weiss to the Pauli (temperature independent) form; inset: electrical resistivity showing the T^2 dependence. (After Andres, K., Graebner, J.E., Ott, H.R., 1975. 4*f* Virtual-bound-state formation in $CeAl_3$ at low temperatures. Physical Review Letter 35, 1979; Steglich, F., *et al.*, 1979. Superconductivity in presence of strong pauli paramagnetism: $CeCu_2Si_2$. Physical Review Letter 43, 1892).

The Mott–Hubbard localization takes place when the magnitude U of the short-range (intra-atomic) repulsive interaction exceeds the average band energy per particle $(1/N)\sum_{k\sigma}\varepsilon_k \equiv \bar{\varepsilon}$. This is because the band energy represents the binding energy gained by forming an extended (Bloch) state of electron in solid, whereas the Coulomb repulsion competes with such a process as it tries to keep the particles as far apart as possible, that is, on their parent atoms (where they are localized).

To put this type of argument on a quantitative basis, the renormalized band energy is represented as $q\bar{\varepsilon}$, where the so-called band narrowing factor is $q \leqslant 1$ and vanishes at the localization threshold. The Coulomb energy (per atom) is written as $U\eta$, where $\eta \equiv \langle n_{i\uparrow}\, n_{i\downarrow}\rangle$ represents the probability that the atomic state 'i' is doubly occupied (a single state per atom is taken, so that the spins are opposite then). When $\eta > 0$, the double occupancies are formed and the electrons (originally one per atom) can hop from one atom onto a neighboring one and thus conduct charge. To close the argument, one specifies $q \equiv q(\eta)$, which in the simplest formulation (the Gutzwiller ansatz) is of the form $q(\eta) = 8\eta(1 - 2\eta)$. Thus, the total energy is

$$E_G/N = q(\eta)\bar{\varepsilon} + U\eta \equiv q(\eta)\sum_{k\sigma}\varepsilon_k + U\eta \qquad [20]$$

In the equilibrium state, $\partial E_G/\partial\eta = 0$, $\partial^2 E_G/\partial\eta^2 > 0$. One then obtains

$$\eta \equiv \eta_0 = \frac{1}{4}(1 - U/U_c) \qquad [21]$$

Author's personal copy

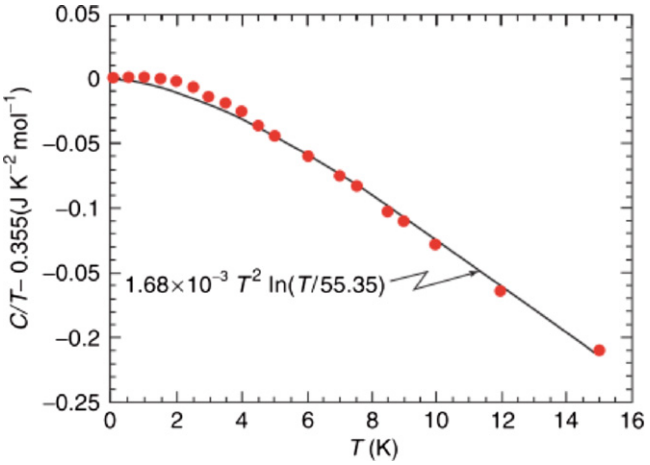

Figure 7 Overall temperature dependence of the (molar) specific heat of $CeRu_2Si_2$, with the linear part extracted. (data: Courtesy of J Flouquet group from Grenoble).

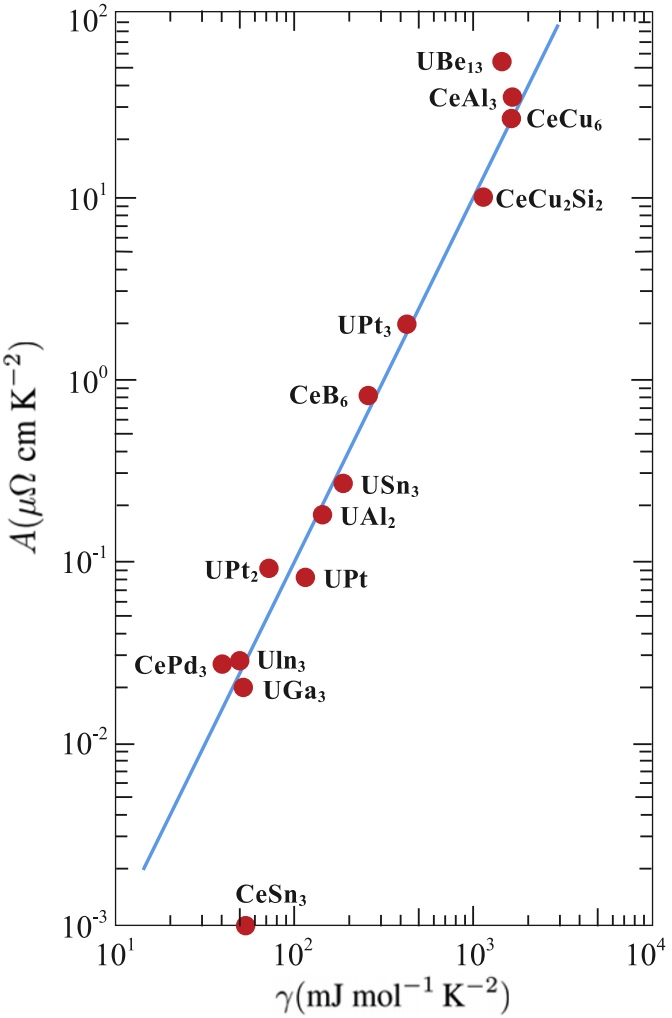

Figure 8 Universal scaling to the A coefficient in resistivity ($\rho(T)=\rho_0+AT^2$) of various heavy fermion systems vs. the coefficient γ_0. The straight line represents the so-called Kadowaki–Woods scaling law $A\sim\gamma^2(0)$ (after Auerbach, A., Levin, K., 1987. Universal low temperature properties of heavy fermion systems. Journal of Applied Physics 61, 3162).

Author's personal copy

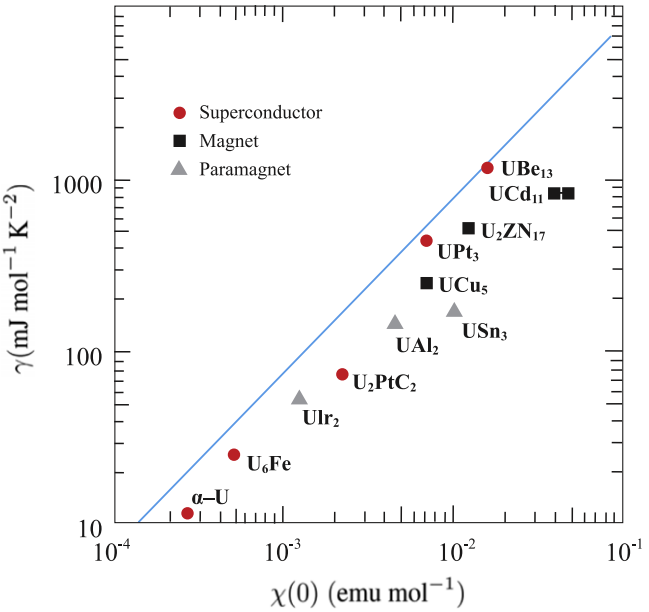

Figure 9 Universal scaling of the coefficient γ_0 vs. the susceptibility χ_0 for various heavy fermion systems. The straight line is for the ideal electron gas. (after Auerbach, A., Levin, K., op. cit).

$$q \equiv q_0 = 1 - (U/U_c)^2 \qquad [22]$$

$$E_G/N = \bar{\varepsilon}(1 - U/U_c)^2 \qquad [23]$$

where $U_c = 8|\bar{\varepsilon}|$ is the critical value of the interaction, at which $E_G = \eta_0 = 0$, that is, the energies totally compensate each other (the metallic state for $U \geqslant U_c$ becomes unstable). One can also calculate the magnitude of spin site on the representative atom that i defined as

$$\langle S_i^2 \rangle = \frac{3}{4}(1 - 2\eta_0) = \frac{3}{8}\left(1 + \frac{U}{U_c}\right) \qquad [24]$$

At $U = U_c$ the spin of the site reduces to the Pauli spin, with $\langle S_i^2 \rangle = \frac{1}{2}\left(\frac{1}{2} + 1\right)$, i.e., to its value in the atomic limit.

A brief interpretation of this new approach with respect to the standard Landau language is in place. Namely, in distinction to the Landau theory, for which the reference state is the ideal electron gas and relevant are the electrons at or in vicinity of the Fermi surface, we now take into account all the system fermions (electrons) into consideration as the local interaction U can reach the magnitude ε_F or be even large. The band narrowing factor q represents a restriction on the motion of individual fermions throughout the system due to the repulsive interaction from the other particles. The reason why the repulsion can be regarded as local (intraatomic) is that now even the itinerant Wannier states are considered near the limit of atomic states overlap is small with the states centered on the neighboring sites. We introduce a quasiparticle language even in that limit as discussed next. For that purpose, we make a brief discussion concerning the transformation of the Fermi liquid into a lattice of localized states, as exemplified by the already introduced Mott–Hubbard transition.

3.3 Mott–Hubbard Transition as a Phase Transition

The factor $q(\eta_0)$ can be interpreted as describing the mass enhancement also. Namely,

$$\frac{m^*}{m} = \frac{\gamma(0)}{\gamma_0} = q^{-1} = \left[1 - \left(\frac{U}{U_c}\right)^2\right]^{-1} \qquad [25]$$

So, m^* diverges (and so does the linear coefficient of the specific heat) as $U \to U_c$ if only the transition is continuous. Additionally, one can also calculate the magnetic susceptibility $\chi(0)$, which reads

$$\chi(0) = \frac{\chi_P}{q(\eta_0)}\left[1 - \frac{U}{U_c}\frac{1 + U/(2U_c)}{(1 + U/U_c)^2}\right]^{-1} \qquad [26]$$

Author's personal copy

where χ_P is the Pauli susceptibility. Note that χ is divergent as $U \to U_c$, since $q \to 0$ in this case (the other factor represents the renormalized Stoner criterion for the onset of ferromagnetism). Hence, the point $U \to U_c$ represents, at least within this simple approach, a quantum critical point (the Brinkman-Rice point). One can also define the parameters F_s^1 and F_a^0 by comparing eqns [25] and [26] with eqns [15] and [17].

3.3.1 Localization of electrons at T > 0 and quasiparticles

One can generalize the meaning of the factor $q(\eta)$ by generalizing the concept of quasiparticle with energies $E_k = q(\eta)\varepsilon_k$. This generalization is basic on the notion that in eqn [20] each of the bare (noninteracting) energy ε_k is reduced (renormalized) by the same factor q. Hence, the statistical distribution of quasiparticles is postulated then, as in the Landau–Fermi liquid, in the form $f(E_k) = \{\exp[\beta(E_k - \mu)] + 1\}^{-1}$. In effect, the free energy of the metallic (delocalized) ALFL written for all fermions is

$$\frac{F}{N} = \frac{1}{N}\sum_{k\sigma} E_k f(E_k) + U\eta + \frac{k_B T}{N}\sum_{k\sigma}\{f(E_k)\ln f(E_k) + [1 - f(E_k)]\ln[1 - f(E_k)]\} \qquad [27]$$

In the low-T limit, the expansion to the first nontrivial order leads to the generalized free energy expression

$$\frac{F}{N} = -q(\eta)\bar{\varepsilon} + U\eta - \frac{\gamma_0 T^2}{2q(\eta)} + o(T^4) \qquad [28]$$

This quantity reduces to the physical free energy at ALFL for the optimal configuration, i.e., for which F has a global minimum as a function of $\eta = \eta(T/U|\bar{\varepsilon}|)$.

The next step is to introduce the discontinuous phase transition in the context of metallic ALFL instability. The localized electrons (atomic $s = 1/2$ spins) are represented in the paramagnetic phase in the simplest manner by their entropic part only, that is, their free energy in the simples case amounts to

$$\frac{F_1}{N} = -k_B T \ln 2 \qquad [29]$$

where the exchange interactions between the electrons have been neglected as only paramagnetic states are discussed here. Equating $F = F_l$, the coexistence of the states regarded as phases in the thermodynamic sense is obtained.

The phase diagram for this system on the plane $T - U/U_c$ is shown in **Figure 10**, together with the 'mean-field' critical points. The main feature is the reentrant (PM) metallic behavior in the high-temperature regime. Such a reentrant behavior is observed for the condensed ^{3}He (on the $p - T$ plane, cf. **Figure 1**). For the canonical Mott–Hubbard electronic system, pure and doped V_2O_3, the upper line $T_+(U)$ represents a crossover behavior accounted for in a more refined approaches (dashed line here).

3.4 Spin-Dependent Quasiparticle Masses and Metamagnetism

There are two unique properties of almost-localized electrons in the presence of magnetic field. The first of them is the itinerant-electron discontinuous transition to metamagnetism, that is, the transition in an applied magnetic field to an almost saturated ferromagnetic phase via a first-order transformation. The metamagnetic transition is companied by a maximum in the linear specific heat coefficient $\gamma(H_a)$. The second is the appearance of a spectacular and unique spin dependence of the quasiparticle masses, with $m^*/m_0 \equiv m_\sigma/m_0 = 1/q_\sigma$, which appears only for a non-half-filled narrow-band situation. In the limit of strongly correlated electrons ($U \gg U_c$), the enhancement factor takes the form

$$1/q_\sigma = (1 - n_\sigma)/(1 - n) \qquad [30]$$

where n is the number of electrons per atom (the band filling) in the correlated band, with the energies of particles $E_k = E_{k\sigma} = q_\sigma \varepsilon_k - \sigma\mu_B H_a$, and n_σ is the number of electrons (per atom) of spin σ (the quantity $\overline{m} \equiv (n_\uparrow - n_\downarrow)/(n_\uparrow + n_\downarrow)$ is the spin polarization per particle). **Figure 11** presents the spin-split masses as a function of $\overline{m}$ for both the majority and the majority-spin subbands for the two-band fillings close to the half-filling, i.e., close to the Mott–Hubbard transition, where localized phase would stabilize. The spin-split masses were predicted first theoretically but have late been detected experimentally in the heavy fermion systems $CePd_2Si_2$ and $CeCoIn_5$ (see Further Reading).

In **Figures 12(a)** and **12(b)** we have plotted the magnetic moment, the double occupancy probability and the spin-split masses, all as a function of the applied field. The numerical results are drown for a two-dimensional square lattice; other parameters: the band filling n is specified and $U/U_c = 0.95$.

Author's personal copy

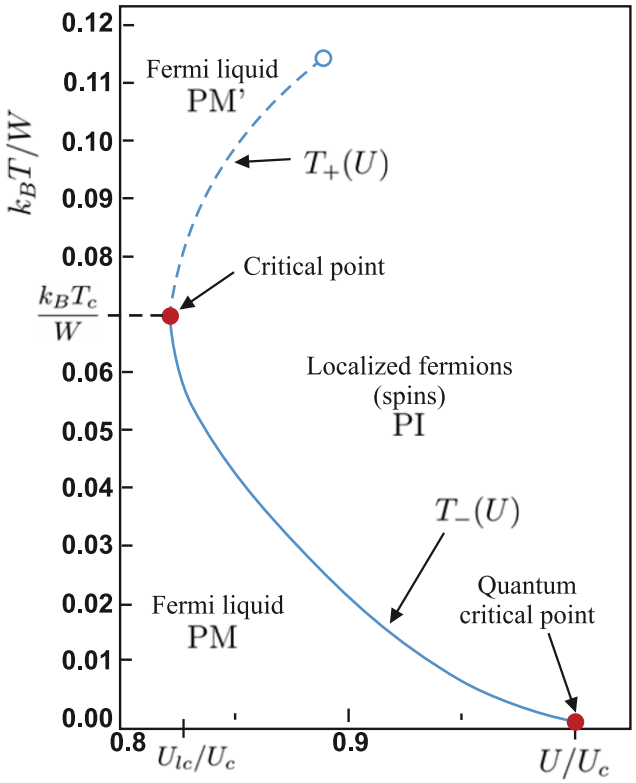

Figure 10 Schematic phase diagram for the almost localized electrons in a narrow band in the paramagnetic state. (After Spałek, J., 2006. Magnetic properties of almost localized fermions revisited: Spin dependent masses and quantum critical behavior. Physica Status Solidi (b) 243, 78).

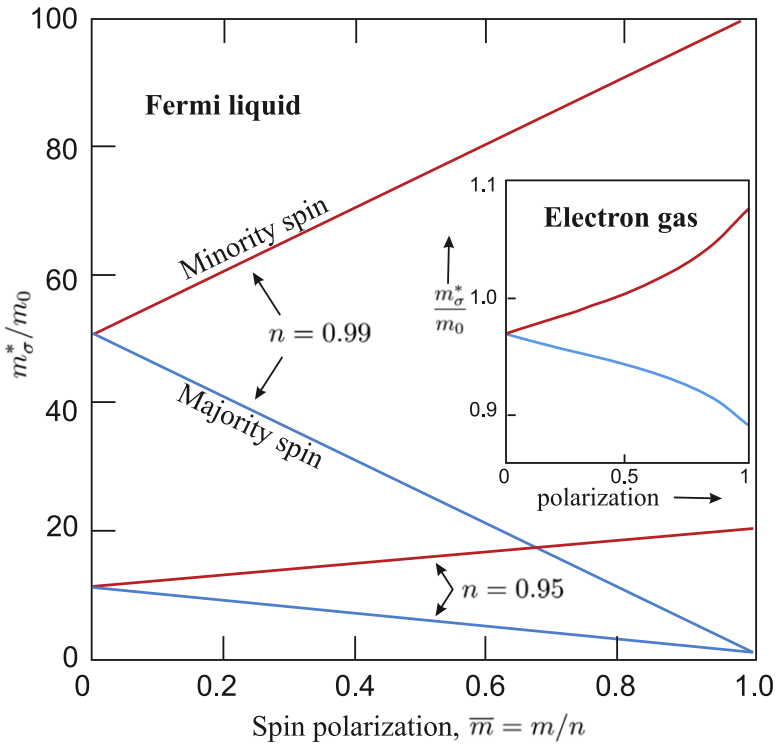

Figure 11 Spin-split effective masses for almost localized electrons as a function of magnetic polarization $\overline{m} = (n_\uparrow - n_\downarrow)/(n_\uparrow + n_\downarrow)$ for the number n of electrons per atom specified. Inset: the same for the polarized electron gas. (After Spałek, J., Gopalan, P., 1990. Almost localized electrons in a magnetic field. Physical Review Letters 64, 2823).

Author's personal copy

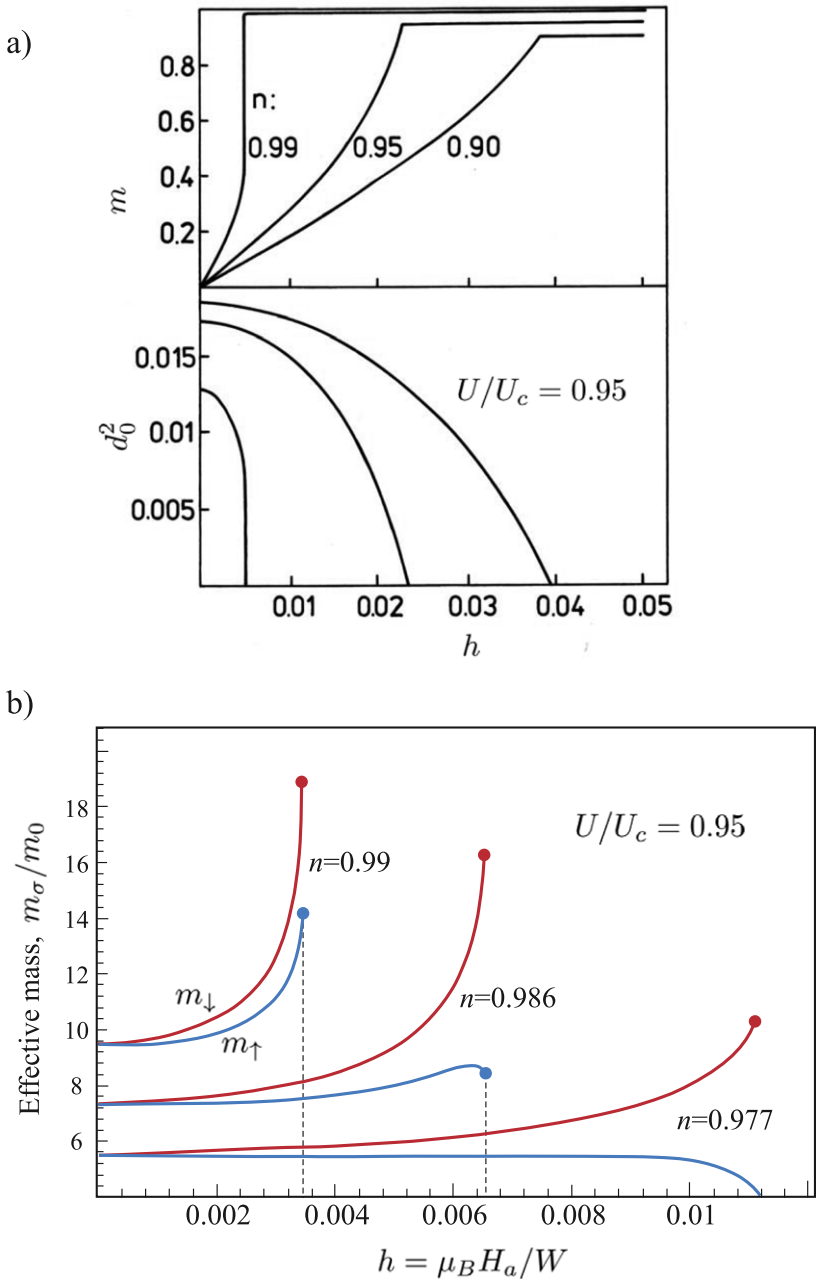

Figure 12 (a) Applied magnetic field dependence of magnetic moment exhibiting the metamagnetic behavior (topmost curves) and the double-occupancy probability d_0^2. (b) The spin dependent masses $m^* \equiv m_\sigma$ relative to the bare (band) mass m_B vs. reduced applied field. The vertical dotted line marks the magnetic saturation limit, at which only the spin-magnetic carriers with $m^* = m_0 = m_B$ survive. (After Korbel, P., 1997. PhD Thesis, Jagiellonian University, Kraków, see: http://th-www.if.uj.edu.plztms/download/phdTheses/Pawel_Korbel_PhD.pdf, Almost Localized Fermi Liquid and its Instabilities Against Mott-Localized and Spin-Liquid States).

3.5 Marginal Fermi Liquid

In the case of a normal FL, one has $\mathrm{Re}\sum(\omega) \sim \omega$, and $\mathrm{Im}\sum(\omega) \sim \omega^2$, whereas in the phenomenological approach to high-temperature superconductors, Varma and co-workers assumed that

$$\sum(\omega) \sim \lambda \left(\omega \ln \frac{\omega_c}{|\omega|} + i|\omega| \right) \qquad [31]$$

Author's personal copy

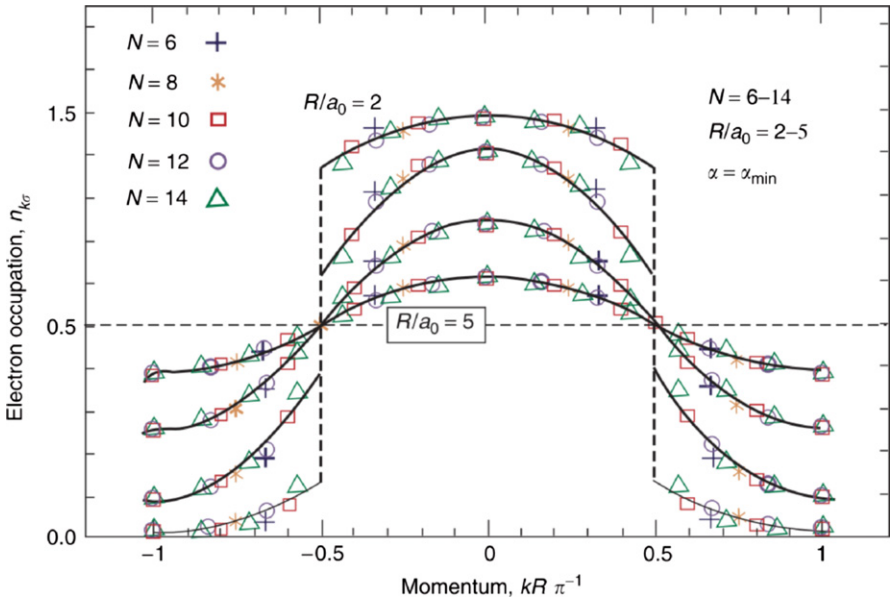

Figure 13 Momentum distribution for interacting electrons in a nanochain of N atoms specified and for different interatomic distances R (in units of 1s Bohr orbit). (cf. Spałek, J., Rycerz, A., 2001. Electron localization in a one-dimensional nanoscopic system: A combined exact diagonalization – An *ab initio* approach. Physical Review B 64, 161105).

and hence the imaginary part is of comparable magnitude to the quasiparticle energies with energies $\omega \sim \varepsilon_{\boldsymbol{k}}$ (λ is the effective coupling constant and ω_c is the so-called cutoff frequency i.e., the energy beyond which the marginal FL (MFL) concept does not hold). The real part of the self-energy is weakly singular and this, in conjunction with the fact that $\sum'' \sim |\omega|$, specifies the two-dimensional nature of those systems. Such phenomenological approach describes roughly the so-called optimally doped high-T_c superconducting systems in the normal state.

3.6 Nanosystems as Quantum Fermi Liquids

In the era of nanotechnology, a legitimate question is: how short can a quantum (monoatomic) wire be? The answer to this question can be provided in the simplest manner by solving exactly the system of $N \sim 10$ atoms with one valence electron (e.g., a chain of N hydrogen or alkali atoms in the simplest situation). Figure 13 shows the statistical distribution function $n_{k\sigma}$ drawn for different interatomic distances R in units of Bohr radius a_0. For $R \approx 2a_0$, the distribution is close to the Fermi distribution, with quasi-discontinuity (the vertical dashed line) near the Fermi point for the infinite system. The distribution is continuous $n_{\boldsymbol{k}\sigma} \approx 1/2$ independent of the particle energy, when the particles become localized on atoms.

4 Beyond the Concept of Fermi Liquid: Quantum Criticality

By quantum phase transition we understand that taking place at temperature $T=0$, i.e., when thermodynamic fluctuations in the equilibrium vanish. This situation raises immediately the basic question that one would think that at $T=0$ the quantum condensed matter is governed by the pure quantum-mechanical laws. But then, what does it actually mean when we cannot solve the $N \to \infty$ problem at hand exactly? In that situation, the concept of spontaneously broken symmetry, introduced for a classical continuous phase transition by Landau, with a concomitant order parameter quantifying that broken symmetry state is still valid albeit of not with as simple meaning, as its classical correspondant. In that situation, the order parameter appears at $T=0$ as a function of the parameter such a external pressure (p) or applied field (H_a) or connection of particles. Obviously, the proper scaling lows around this quantum critical point (QCP) must also involve the limit $T \to 0 (T>0)$ to determine the quantum critical properties distinct from the near the classical critical point (CP). The basic question is what exactly induces the symmetry breakdown at $T=0$? We are interested here in an itinerant (correlated) fermionic liquids. In that situation, at least in the case of Mott–Hubbard localization, it involves a competition between the kinetic (renormalized band) favoring energy of the delocalized states, and the repulsive interparticle interaction favoring the localized (quasiatomic) states. We have seen it earlier, where at $U=U_c$ the kinetic ($q\bar{\varepsilon}<0$) and the interaction ($U\eta>0$) parts compete and compensate each other exactly for $U=U_c$. At $T=T_{\mathrm{MIT}}>0$ the difference in entropy (thermodynamic factor) plays the role of the tip-of-balance in the situation when the above two energies almost balance out each other. The second example is provided by the heavy fermion systems in which there is a subtle

Author's personal copy

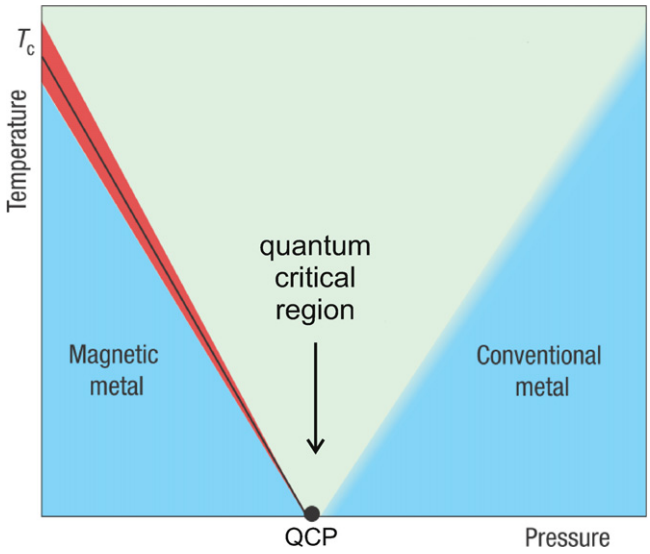

Figure 14 A schematic phase diagram on pressure–temperature plane with a quantum critical point (QCP) in between magnetic and normal metallic states. The region in red corresponds to classical regime, the quantum critical regime, where usually temperature dependence of physical quantities appears is also marked (cf. **Table 2**). (After Lanzarich, G.G., 2005. Magnetic quantum liquid enigma. Nature Physics 1, 11).

Table 2 Spin-fluctuation scenario at QCP: temperature dependence of physical quantities for $T\to 0$ (courtesy of Dariusz Kaczorowski); a and T_0 are constants

Dimension		*Specific heat coeff.*, C/T	*Electrical resistivity*, $\Delta\rho$	*Magnetic susceptibility*, $\Delta\chi$
$d=3$	FM ($z=3$)	$\sim \log T_0/T$	$\sim T^{5/3}$	$\sim T^{-4/3}$
	AFM ($z=2$)	$\sim 1 - aT^{1/2}$	$\sim T^{3/2}$	$\sim T^{-3/2}$
$d=2$	FM ($z=3$)	$\sim T^{5/3}$	$\sim T^{3/2}$	$\sim T^{-1}/\log T$
	AFM ($z=2$)	$\sim \log T_0/T$	$\sim T$	$\sim (\log T)/T$

counterbalance between a weak magnetic ordering or spin fluctuations and the onset of superconductivity, particularly if it takes the form of spin-singlet superconductivity, in which case it takes the form of a competition between the local dynamic magnetic excitations and their non-magnetic (Cooper pairs) correspondants.

Let us characterize briefly QCP in general terms. In **Figure 14** we draw schematically the phase diagram involving a quantum critical point. What is important, in the quantum critical regime marked on the Figure the temperature dependence of the properties in the low-T limit are completely different than the corresponding properties for the Fermi liquid discussed earlier (in which we had integer exponents, i.e., quantities $\sim T$ or to $\sim T^2$ only). The difference is displayed schematically in **Table 2** for the systems of dimensionality $d=3$ and for system close to ferromagnetic (FM) and anti-ferromagnetic (AFM) instability. Appearance of the dynamic exponent stems from the circumstance that in the case of quantum phase transition ($T\to 0$), a nontrivial dynamics (time dependence) arises and is entangled with the ordinary thermodynamic spin fluctuation processes. The logarithmic term appeared already when the collective spin fluctuations are included (cf. **Figure 6**). Near the quantum continuous transition we observe additionally that the single-particle dynamics (manifested by the term γT in the specific heat) becomes overshadowed by the singular collective (e.g., spin) fluctuations.

5 Extension of the Fermi-Liquid Concept: Magnetism and Superconductivity

Expression [4] can be generalized to include not only particle–particle density interaction, but also the spin–spin exchange interaction, where the second term is changed to the spin-rotationally invariant form.

$$f^{\sigma\sigma'}_{\mathbf{k}\mathbf{k}'} = f^s\left(\mathbf{k}\cdot\mathbf{k}'/k_F^2\right) + \boldsymbol{\sigma}\cdot\boldsymbol{\sigma}' f^a\left(\mathbf{k}\cdot\mathbf{k}'/k_F^2\right) \qquad [32]$$

where $\boldsymbol{\sigma}\equiv(\sigma_x,\sigma_y,\sigma_z)$ denotes the Pauli matrices. In the broken symmetry state the latter term introduces generally an effective field which introduces a uniform spin splitting if $f^a<0$ and thus can lead to a Stoner quantum critical point (QCP) for $F_0^a=-1$ as

Author's personal copy

signaled by the form of the magnetic susceptibility (cf. eqn [17]) divergence at $T=0$. For $F_0^a \lesssim -1$ we have a weak ferromagnetic state with strong spin fluctuations of the small static moment already at low temperatures, as the Curie temperature $T_c \sim |F_0^a - 1| \to 0$. We are thus entering the quantum critical regime outlined above. It can be modeled by the Hubbard model from which the scattering function of the form [11] or [32] can be derived (cf. Vollhardt, 1984).

The situation is quite different in description of superconductivity. In the simplest case of the Bardeen–Cooper–Schrieffer (BCS) theory the pairing is taking place in $\boldsymbol{k}$ space, so the Landau quasiparticles picture can be directly adopted to that case. However, the density–density (including spin–spin) form of correlation functions is insufficient in this case. In general, the particle-number non-conserving term must be added, to the particle–particle interaction which in turn introduces a gap in the single-particle spectrum of individual quasiparticles representing the exited states from the condensed (paired-particle) state. The state is still metallic. Therefore, the particle current in such condensed state is composed of a coherent (with the same phase) supercurrent of the pairs. Note that almost vertical lines locked up at $T=T_N$ and $T=T_s$ in the range of 1 mK in **Figure 1** represent the (antiferro-) magnetic and paired (superfluid) transition lines for ^{3}He in the solid and liquid phases, respectively. So, even in this canonical Fermi fluid those two types of ordering appear in addition to the Mott transition (solidification). A further analysis of those points requires a separate and thorough discussion.

6 Outlook

The concept of the Fermi liquid is very useful in rationalizing the temperature, pressure, applied magnetic field data for many metallic materials and on this basis, determining the principal characteristics. The concept can be extended to describe some classes of superconductors (classical BCS superconductor) and itinerant ferro- and antiferro- magnets, although in most of the cases inclusion of interelectronic correlations is important if not indispensable. The rule of thumb in singling out a specific metal as a Landau-type Fermi liquid is: a relatively high value of the linear specific-heat coefficient ($\gamma_0 \sim 10$ mJ mol K^{-2} or more), a relatively high value of the paramagnetic susceptibility $\chi \gtrsim 10^{-3}$ emu, and the carrier effective masses m^* obtained from, for example, de Haas-von Alphen method in the range of $2 \div 10\, m_0$. In the correlated systems $\gamma \gg \gamma_0$ which means that the electronic entropy represents an important part of total entropy, temperature dependence of resistivity $\rho(T)$ has a large $\sim T^2$ term and the $m^*/m_0 \gg 1$. It is absolutely amazing that FL concept is applicable to the metallic heavy – electron systems with the effective electron masses $m^*/m_0 \sim 10^2 \div 10^3$ (i.e., reaching that of proton or neutron at rest). Equally amazing is the circumstance that their Fermi energy $\varepsilon_F = \varepsilon_F^0(m_0/m^*) \ll \varepsilon_F^0$ so that it must be characterized in Kelvin units, since $T_F \equiv \varepsilon_F/k_B \sim 10 \div 10^2$ K. The principal physics of Landau Fermi liquids is well established, so the present research in this area has shifted to the study of strongly correlated systems and those with *a quantum criticality non-Fermi liquids* (NFL). The last subject is the process of intensive studies. **Figure 14** illustrates a typical phase diagram on the pressure–temperature plane at the border of magnetism in heavy-fermion compounds. In **Table 2** we show typical singular type of behavior observed in those systems close to QCP and $T \to 0$.

Acknowledgments

The work was partly supported by the Foundation for Polish Science (FNP) under the Grant TEAM and partly by the National Science Centre (NCN) under MAESTRO, Grant No. DEC-2012/04/A/ST3/00342. Technical help of Dr. Danuta Goc-Jagło is greatly appreciated.

References

Mook, H.A., 1985. Momentum distribution of ^{3}He. Physical Review Letters 55, 2452.
Vollhardt, D., 1984. Normal ^{3}He: An almost localized Fermi liquid. Reviews of Modern Physics 56, 99.

Further Reading

The Landau theory of Fermi liquids, both phenomenological and its microscopic justification, is elaborated in classic works:

Abrikosov, A.A., Gorkov, L.P., Dzialoshinski, J.E., 1963. Methods of Quantum Field Theory in Statistical Physics. New York: Dover (Chapters 1 and 4).
Electrons in metals are discussed in detail: Abrikosov, A.A., 1988. Fundamentals of the Theory of Metals. Amsterdam: North-Holland.
For exposition including later applications see: Baym, G., Pethick, C., 1991. Landau Fermi-Liquid Theory. New York: Wiley.
Liquid – ^{3}He properties have been overviewed by experimentally and theoretically in: Dobb, C., 2000. Helium Three. Oxford: Oxford University Press; The connection of the Fermi-liquid theory with the prediction of the Hubbard model is provided in: Vollhardt, D., 1984. Normal ^{3}He: An almost localized Fermi liquid. Reviews of Modern Physics 56, 99.
Pines, D., Nozieres, P., 1988. The Theory of Quantum Liquids, second ed. Redwood City: Addison-Wesley.

Author's personal copy

Spałek, J., 2000. Correlated Fermions: A New Paradigm in Physics on the Example of Solid State Physics. European Journal Physics 21, 511–534; Honig, J.M., Spałek, J., 1998. Electronic properties of $NiS_{2-x}Se_x$ single crystals: From magnetic Mott–Hubbard insulators to normal metals. Chemistry of Materials 10, 2910–2929.

The spin-direction dependent effective masses of quasiparticles were discuss in: Sheikin, I., *et al*., 2003. High magnetic field study of $CePd_2Si_2$. Physical Review B 67, 094420; McCollam, A., 2005. Anomalous de Haas – van Alphen Oscillations in $CeCoIn_5$. Physical Review Letters 94, 186401; for review see: Spałek, J., 2006. Magnetic properties of almost localized fermions revisited: Spin dependent masses and quantum critical behavior. Physica Status Solidi (b) 243, 78–88.

Provided for non-commercial research and educational use.
Not for reproduction, distribution or commercial use.

This article was originally published in the *Reference Module in Materials Science and Materials Engineering*, published by Elsevier, and the attached copy is provided by Elsevier for the author's benefit and for the benefit of the author's institution, for non-commercial research and educational use including without limitation use in instruction at your institution, sending it to specific colleagues who you know, and providing a copy to your institution's administrator.

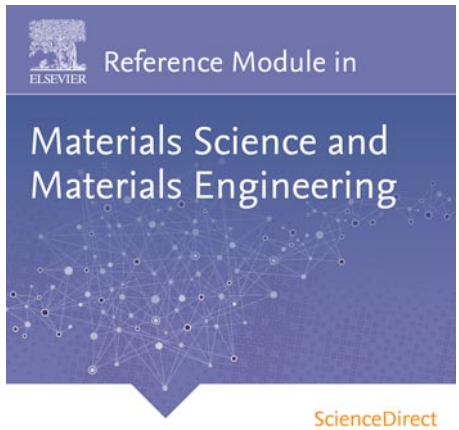

All other uses, reproduction and distribution, including without limitation commercial reprints, selling or licensing copies or access, or posting on open internet sites, your personal or institution's website or repository, are prohibited. For exceptions, permission may be sought for such use through Elsevier's permissions site at:

http://www.elsevier.com/locate/permissionusematerial

Spalek J., Liquids, Theory of: Fermi Liquids. In: Saleem Hashmi (editor-in-chief), Reference Module in Materials Science and Materials Engineering. Oxford: Elsevier; 2016. pp. 1-20.

ISBN: 978-0-12-803581-8
Copyright © 2016 Elsevier Inc. unless otherwise stated. All rights reserved.